Radiological Physics and Technology (2019) 12:283–289
https://doi.org/10.1007/s12194-019-00519-5

# Determination of appropriate conversion factors for calculating size-specific dose estimates based on X-ray CT scout images after miscentering correction

**Marin Terashima[1] · Kazufusa Mizonobe[2,4] · Hiroyuki Date[3]**

Received: 19 December 2018 / Revised: 4 June 2019 / Accepted: 5 June 2019 / Published online: 20 June 2019


**Abstract**
In this study, we proposed and evaluated the validity of an optimized size-specific dose estimate, a widely used index of radiation dose in X-ray computed tomography (CT) examinations. Based on miscentering correction of scout images, we determined the appropriate conversion factors (CF) by using a phantom. Scans were conducted using a multi-detector CT system (Aquilion ONE, Canon Medical Systems). Four cylindrical phantoms were taken in the anteroposterior (AP) and axial directions to determine the relationship between pixel value and water-equivalent length ($L_w$). In the AP scout image, the pixel values at the selected slice positions were converted to $L_w$ to calculate the water-equivalent diameter ($D_w$). The CF was derived from $D_w$ and CF values before and after miscentering correction was calculated. Finally, the CF values were compared to those calculated from the axial image using the conventional methodology of the American Association of Physicists in Medicine. Before miscentering correction, the maximum difference between the CF values of the axial and scout images was 7.26%. However, after miscentering correction, the maximum difference was 1.34%. Validation using a whole-body phantom generally revealed low maximum differences between the CF from the axial image and the values from the miscentering-corrected scout images. These were 2.41% in the chest, 6.30% in the upper abdomen, 1.43% in the abdomen, and 2.45% in the pelvic region. Consequently, we concluded that our miscentering correction method for deriving the appropriate CF values based on scout images is advantageous.

**Keywords** Size-specific dose estimate · Computed tomography dose index · Miscentering correction

## 1 Introduction

The recent popularization of multi-detector computed tomography (CT) has coincided with an increase in clinical CT examinations. The radiation dose from CT is generally higher than that from other diagnostic modalities; thus, it requires careful and appropriate evaluation. The volume CTDI ($CTDI_{vol}$) is widely used as a radiation dose index during CT examinations and is displayed on the console of CT scanners. $CTDI_{vol}$ is obtained from measurements using 16-cm- and 32-cm-diameter and 15-cm-long reference phantom; these values are often measured using an ion chamber dosimeter. However, the $CTDI_{vol}$ does not account for patient size and only provides information about scanner output for a very specific standardized condition [1]. Thus, the size-specific dose estimate (SSDE) proposed by the American Association of Physicists in Medicine (AAPM), which permits estimates based on individual patient size, has gained widespread acceptance as an alternative CT radiation dose index [2–7]. SSDE is defined by the product of the $CTDI_{vol}$ and a correction factor (CF) for patient size. Here, the CF is characterized by an effective diameter ($D_{eff}$) [2] that can be calculated from the diameter of image landmarks such as lateral (LAT) projection, anteroposterior (AP) projection, a combination of the two projections, or the effective area

✉ Hiroyuki Date
date@hs.hokudai.ac.jp

Marin Terashima
marinsan.0429@gmail.com

1 Graduate School of Health Sciences, Hokkaido University, Sapporo, Japan

2 Division of Radiology and Nuclear Medicine, Sapporo Medical University Hospital, Sapporo, Japan

3 Faculty of Health Sciences, Hokkaido University, Sapporo, Japan

4 Present Address: Department of Radiation Oncology, Kobe Minimally Invasive Cancer Center, Kobe, Japan

($A_{ROI}$) of the patient's cross section. However, $D_{eff}$ does not account for the attenuation of X-ray photons arising from tissue density variations within the patient's body. For example, the lung is less dense than the abdominal organs, and the thorax would attenuate fewer X-ray photons compared with the abdomen at the same imaging parameters. To manage these variations, the water-equivalent diameter ($D_w$) was proposed to express X-ray attenuation by the patient's body in a manner equivalent to a cylindrical water phantom having the same X-ray absorption; therefore, it provides accurate size-corrected dose estimates [8, 9]. AAPM Report 220 proclaimed that the use of $D_w$ is a preferred method for determining the SSDE correction factors [10].

Conventionally, $D_w$ and CF are determined from CT axial images. However, a fundamental disadvantage of axial images is the occasional presence of truncations in the outline of the patient due to the small field of view (FOV) of certain images (e.g., cardiac CT); this can make it difficult to deduce the SSDE. Another disadvantage is that they cannot be obtained before scanning. Hence, to avoid these problems, scout images can be used, although some drawbacks include the magnification (or demagnification) of the images with respect to the patient due to miscentering, and the inability to perform Hounsfield unit scale transformations. However, miscentering can be corrected using a histogram of the selected slice position from the LAT scout image [11], and simple alternative scale transformation methods have been proposed based on the linear relationship between pixel values and the $L_w$ value [9, 12, 13]. Nevertheless, histograms derived from scout images tend to have irregular distributions depending on the CT scanner type, and the area scanned (especially the chest), which leads to poor outcomes.

Although using scout images may have drawbacks compared to using axial images, the former is appealing due to the avoidance of truncation. Moreover, if the drawbacks of using scout images are appropriately addressed, more useful advantages could be attained. Scout images are taken clinically to determine the position of the axial image acquisition and to activate auto exposure control (AEC), which adjusts the dose according to the body thickness. Even though a certain dose quantity is necessary to obtain the scout image, the patient's final radiation dose is reduced by determining the minimum scanning range and activating the AEC. However, miscentering at the time of obtaining the scout image incorrectly influences the tube's current adjustment by the AEC. Hence, if this problem is improved, the AEC will start up correctly and result in a lowered overall radiation dose for the patient [14].

By overcoming the drawback of miscentering through the establishment of an optimized SSDE method, this study sought to harness the potential advantages of using scout images. In summary, we corrected miscentering and subsequently used the Digital Imaging and Communications in Medicine (DICOM) tag information to determine the optimum CF based on a miscentering-corrected CT scout image. The results were compared to those based on the method proposed by the AAPM report 220, and the validity of the proposed method was evaluated using a whole-body phantom.

## 2 Materials and methods

### 2.1 CT scanner and phantoms

CT scans were performed on multi-detector CT systems (Aquilion ONE, Canon Medical Systems, Otawara, Japan, and partly LightSpeed VCT VISION, GE Healthcare, Milwaukee, WI, USA). Four cylindrical water phantoms with diameters of 6.6, 19.5, 25.5, and 33.5 were used to correlate pixel values of images with the water-equivalent length ($L_w$). The 25.5-cm-diameter phantom was also used to investigate the usefulness of miscentering correction. The appropriate CF values for the SSDE values were determined with reference to the trunk of the PBU-50 (Kyoto Kagaku) phantom (Fig. 1).

### 2.2 Conventional CF determination via axial images

The AAPM's recommended SSDE method was established in 2011 as an index of radiation dose on X-ray CT images. The SSDE value is expressed as a product of the previous index ($CTDI_{vol}$) and CF as:

$$SSDE = CTDI_{vol} \times CF. \quad (1)$$

The CF can be obtained by first considering the volume of the patient to be scanned as a water-equivalent cylinder. The area of the circle at the axial end of that cylinder is sized to encompass the tissue targeted in the axial CT image and is referred to as the water-equivalent area ($A_w$). As shown in the AAPM report, $A_w$ can be

**Fig. 1** The trunk of the PBU-50 (Kyoto Kagaku) phantom

calculated using the mean CT number within a region of interest (ROI) as:

$$A_{\mathrm{w}} = \left( \frac{\overline{\mathrm{CT}(x,y)_{\mathrm{ROI}}}}{1000} + 1 \right) \times A_{\mathrm{ROI}}, \tag{2}$$

where $\overline{\mathrm{CT}(x,y)_{\mathrm{ROI}}}$ is the mean CT number in the ROI and $A_{\mathrm{ROI}}$ is the total area of the ROI ($= \sum A_{\mathrm{pixel}}$). $D_{\mathrm{w}}$ is the diameter of the circle comprising $A_{\mathrm{w}}$ and is thus calculated as:

$$D_{\mathrm{w}} = 2\sqrt{\frac{A_{\mathrm{w}}}{\pi}}. \tag{3}$$

Finally, CF can be calculated using the following equation as in the AAPM report No. 220,

$$\mathrm{CF} = a \times e^{-b \times D_{\mathrm{w}}}, \tag{4}$$

where $a = 3.704369$ and $b = 0.036719$. In this study, CF is based on a 32-cm-diameter CTDI body phantom.

## 2.3 Scout image-based miscentering characteristics and correction

The primary limitation to the AAPM's approach using axial images is the small FOV, which can truncate the patient's outline and make the $A_{\mathrm{ROI}}$ and SSDE difficult to establish. Scout images can be used to avoid this limitation, albeit with the drawback that if the patient/phantom is miscentered higher (or lower) on the y-axis than the isocenter of the CT scanner, the AP scout image is magnified (or demagnified) with respect to the patient/phantom (Fig. 2).

In this study, miscentering was corrected using the LAT scout image. First, we evaluated the amount of miscentering ($\Delta d$) between the phantom center and the isocenter of the CT scanner using the LAT scout image (Fig. 3). The phantom center position was defined as the midpoint between its anterior and posterior ends. The y-axis value ($y$ value) on the anterior side of the phantom was estimated via image thresholding. The $y$ value on the posterior side was set equivalent to the height of the bed displayed in the DICOM tag. The phantom center can be calculated by calculation of the difference

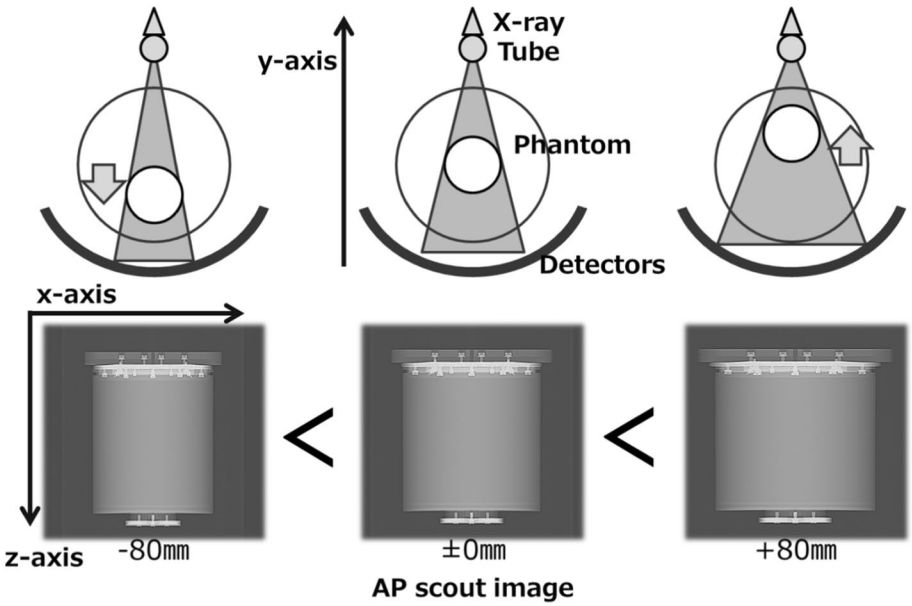


**Fig. 2** Magnification or demagnification according to isocenter location. *AP* anteroposterior

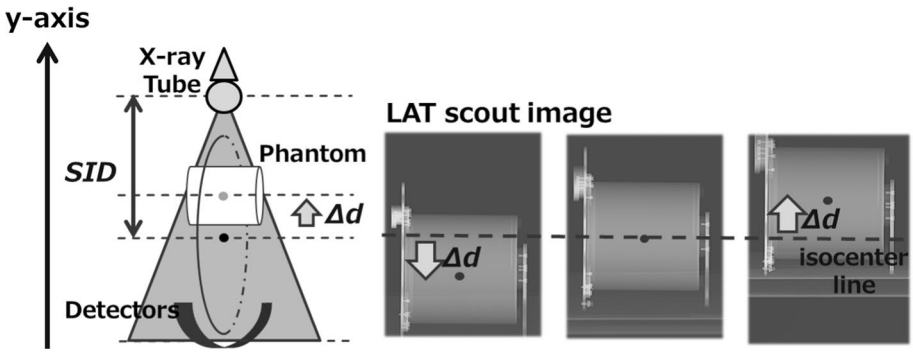


**Fig. 3** Miscentering ($\Delta d$) the phantom center from the isocenter on LAT scout images. *LAT* lateral, *SID* source to isodistance

between the anterior and posterior $y$ values. The y value of the isocenter is equivalent to the center of the LAT scout image. Thus, $\Delta d$ is calculated as the difference between the phantom center and the isocenter. Here, $\Delta d$ is assumed to be positive in the direction of the X-ray tube and negative in the direction of the detector. Finally, the magnified (or demagnified) scout width (SW) on the AP image can be corrected to the correct width (CW) according to the following equation, which is based on the similarity rule of the object:

$$\mathrm{CW} = \frac{\mathrm{SID} - \Delta d}{\mathrm{SID}} \times \mathrm{SW}, \tag{5}$$

where SID stands for source to isodistance. SW can be obtained from the pixel width of the phantom in the AP scout image.

### 2.4 Pixel value and $L_w$ in the scout image

The four cylindrical phantoms were scanned in the AP and axial directions to determine the relationship between pixel value and $L_w$. Based on the AP scout image, the mean pixel value within a 4 × 10-pixel x–z axis rectangle at the center of the phantom was determined. On the axial image, the $L_w$ value at the center of the phantom was measured manually (Fig. 4). The results for both values are given in Table 1 for each phantom size. An excellent linear relationship between them is apparent in Fig. 5.

### 2.5 Scout image-based CF calculation following miscentering correction

The pixel value reportedly increases linearly with increasing $L_w$ [9]. In this study, the relationship between the mean pixel value and $L_w$ was obtained by plotting the manually derived $L_w$ values and pixel values from Table 1 and calculating the regression line. The resulting regression equation was as follows:

$$L_w = 0.162563 \times \text{mean pixel value} - 1.506170. \tag{6}$$

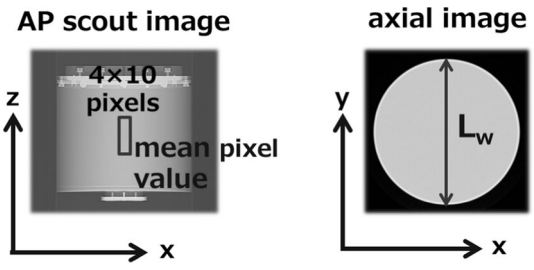


**Fig. 4** AP and axial scout images of a cylindrical phantom, respectively, depicting the area for determining the mean pixel value (left) and $L_w$ (right). *AP* anteroposterior, $L_w$ water-equivalent length

**Table 1** Mean pixel value and $L_w$ according to phantom size

| Phantom diameter (cm) | Mean pixel value | $L_w$ (cm) |
|---|---|---|
| 6.6 | 49.93 | 6.62 |
| 19.5 | 129.73 | 19.53 |
| 25.5 | 165.63 | 25.47 |
| 33.5 | 215.5 | 33.52 |

$L_w$ water-equivalent length

A row of pixels from the AP scout image was selected, and their pixel values were converted to $L_w$ using Eq. 6. Next, $A_w$ was calculated as the product of the mean $L_w$ ($\overline{L_w}$) for all pixels in the selected row and CW as:

$$A_w = \overline{L_w} \times \mathrm{CW}. \tag{7}$$

Finally, CF values were calculated using Eqs. 3 and 4. For this study, the 25.5-cm cylindrical phantom was set at the following bed heights: −80 mm, −40 mm, 0 mm, +40 mm, and +80 mm. Subsequently, the pre- and post-miscentering correction CF values were calculated for each of these bed heights. The resulting CF values were compared with the CF values that were conventionally calculated via the AAPM methodology from the axial image (2.2).

### 2.6 Validation of CF using a trunk part of the PBU-50 phantom

To evaluate the validity of our scout image and miscentering correction method, a trunk phantom was scanned with its center at the isocenter of the CT scanner. Extraction of rows in the scout image was made corresponding to the slice position obtained from the DICOM header of the axial image. CF values were calculated from the axial image without any truncation at each slice position via the conventional AAPM methodology, thus permitting comparison with the scout image-based CF values calculated at the same slice positions.

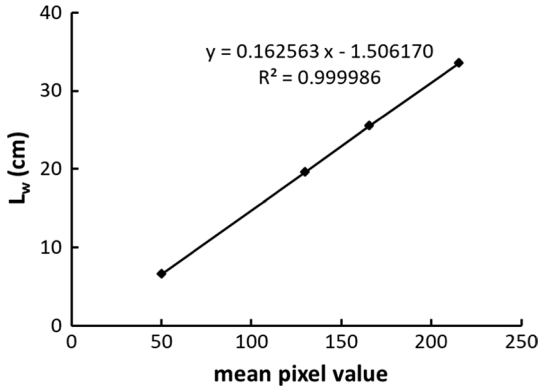


**Fig. 5** Relationship between the mean pixel value and water-equivalent length ($L_w$)

**Table 2** AP scout image CF values before and after miscentering ($\Delta d$) correction and percent difference from axial image CF (1.450) with Aquilion ONE

| Bed Height (mm) | $\Delta d$ (mm) | CF before correction | Difference (%) | CF after correction | Difference (%) |
|---|---|---|---|---|---|
| − 80 | − 82.520 | 1.555 | 7.264 | 1.461 | 0.758 |
| − 40 | − 42.480 | 1.513 | 4.380 | 1.460 | 0.693 |
| 0 | − 1.470 | 1.467 | 1.185 | 1.458 | 0.585 |
| 40 | 39.551 | 1.430 | − 1.372 | 1.469 | 1.342 |
| 80 | 77.637 | 1.373 | − 5.296 | 1.460 | 0.725 |

*AP* anteroposterior, *CF* correction factor

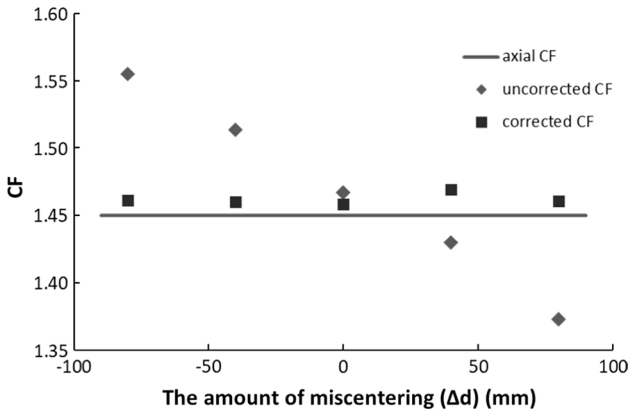


**Fig. 6** Pre- and post-correction AP scout image CFs according to miscentering ($\Delta d$) amount. $\Delta d$ is plus-signed toward X-ray tube and minus toward detector

## 3 Results

### 3.1 Evaluation of the usefulness of miscentering correction

The CF calculated from the axial image was 1.450. Table 2 and Fig. 6 show the results for the amount of miscentering ($\Delta d$) from the LAT scout image, pre- and post-miscentering correction AP scout image CF values, the CF of the axial image, and the percent differences between the axial CF and the pre- and post-corrected AP scout image CF values. The amount of miscentering is plus-signed toward the X-ray tube and minus-signed toward the detector. Before miscentering correction, the percentage differences between the axial image CF and the AP scout image CF values ranged up to 7.26%. After miscentering correction, the maximum percentage difference in CF was reduced to 1.34% (Table 2, Fig. 6). By miscentering correction, the CF value was almost constant regardless of the bed height. This trend was also confirmed for LightSpeed VCT VISION (GE Healthcare).

### 3.2 Evaluation using a trunk phantom

Figure 7 shows the results of the CF values from the axial image and the AP scout image at each slice position of the trunk phantom as well as the difference between them. The differences between the CF from the axial image and those from the scout images of the trunk phantom were small in all slices. The maximum differences were 2.41% in the chest, 1.43% in the abdomen, and 2.45% in the pelvic region. However, in the upper abdominal region, the maximum difference was relatively high at 6.30% (Fig. 7).

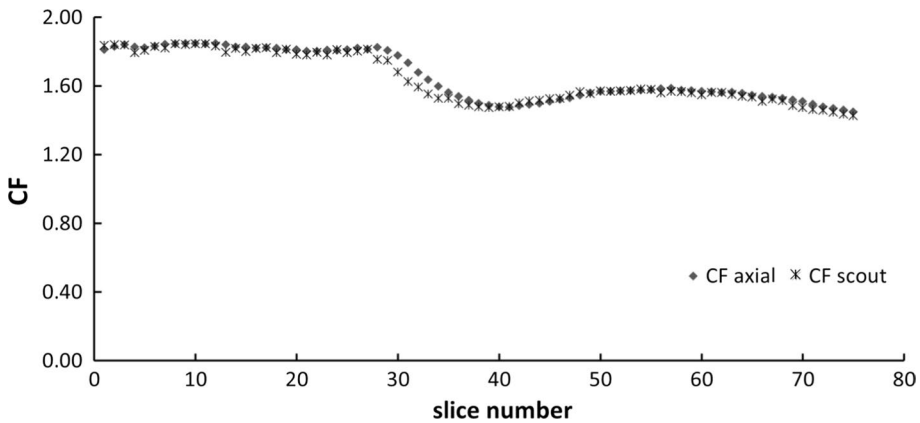


**Fig. 7** Comparison of the CF values (along the z-axis) from the axial computed tomography image and the AP scout image for the trunk phantom. *CF* correction factor, *AP* anteroposterior

## 4 Discussion

Table 2 shows that AP scout image-based miscentering can be corrected using the method proposed in this study. The anterior position of the phantom is easily or automatically extracted via processing steps such as image thresholding by using LAT scout image. However, extraction of the posterior position of the phantom is greatly influenced by the bed, which may or may not be radiographed in the scout image depending on its height. In such a case, it is difficult to extract the accurate position based on the histogram of the pixel value from the LAT scout image. It is particularly difficult to automatically extract the position of the bed in the chest region because the histograms around the chest tend to present irregular (scattering) distributions [11]. To overcome this, we established a relationship between the tag information of the bed height on the DICOM and the position coordinate in the image. Our results indicated that this relationship is linear and similar to that exhibited by another CT scanner (LightSpeed VCT VISION; GE Healthcare, Milwaukee, WI, USA). Using this relationship, we could accurately extract the posterior position of the phantom.

Our results clarified that magnification (or demagnification) increases as the amount of miscentering increases (Fig. 6); this finding is analogous to the result of the AAPM report 220 [10]. Using our proposed method to correct this miscentering, the percentage difference between the axial image CF and AP scout image CF was reduced. Furthermore, the validation of our method using the trunk phantom revealed that post-correction CF values correlated with the axial image CF at almost every site, even though a slight difference appeared around the upper abdomen (slice number around 30 in Fig. 7). It was unclear what caused this difference. However, AAPM task group 220 reports that if the difference between the pre- and post-scan (scout and axial image) values for $D_w$ and SSDE is shown to be consistently less than 10% of the pre-scan values across a range of patient size and habitus, the pre-scan values can be used as the final values [10]. Thus, we concluded that the use of the value from the AP scout image is fair.

We also calculated $D_w$ and CF values based on the linear relationship between pixel value and $L_w$ using scout images. As previously reported, pixel value increased linearly with increasing $L_w$ [9, 12]. However, because the slope and intercept of this linear function are largely dependent on the type of CT scanner used, others attempting to use our method will first need to establish the relationship between the pixel value and $L_w$ for their respective CT scanners. It will also be necessary to confirm the linear correlation between the tag information of the bed height on the DICOM and the coordinate position of the image.

The miscentering correction method proposed in this study requires scanning the LAT scout image and an AP scout image, a deviation from the conventional protocol. More accurate CF before scanning would enable us to perform the scanning with more appropriate doses. This implies that the benefits outweigh the risks of radiation in terms of radiation protection practices. However, a limitation of this method is the reduced correction accuracy when the patient is decentered along the LAT direction.

Because the trunk phantom used to validate our method is rather homogeneous in density compared with the actual human body, further validation using actual clinical images is needed.

## 5 Conclusion

In this study, we proposed and validated a method to correct the problem of magnification (or demagnification) that occurs due to miscentering when AP scout images are used to obtain the CF for SSDE from a CT scan. Our method corrected miscentering by using an LAT scout image. Using a cylindrical phantom, the maximum percentage difference between the CF values calculated conventionally from an axial image and those calculated from AP scout images was reduced from 7.26 to 1.34% after correcting for miscentering using our method. The examination using a trunk phantom revealed that the percentage differences between the CF values from an axial image and the corrected AP scout images were small at almost every site, reaching a maximum of 6.30%. Considering the accuracy of our method compared to that of a conventional axial image-based CF calculation and the fact that scout images are less likely than axial images to be truncated, the scout image-based CF calculation method may be advantageous even for clinical applications.

**Acknowledgements** The authors thank Dr. Jared Boasen, Research Associate of Faculty of Health Sciences in Hokkaido University, for correcting our English expressions.

### Compliance with ethical standards

**Conflict of interest** The authors declare that they have no conflict of interest.

**Ethical approval** The article does not contain any studies with human participants or animals performed by any of the authors.

## References


1. McCollough CH, Leng S, Yu L, Cody DD, Boone JM, et al. CT dose index and patient dose: they are not the same thing. Radiology. 2011;259:311–6.
2. American Association of Physicists in Medicine. Size-specific dose estimates (SSDE) in pediatric and adult body CT examinations. Report of AAPM Task Group 204, 2011.
3. Kidoh M, Utsunomiya D, Oda S, Nakamura T, et al. Breast dose reduction for chest CT by modifying the scanning parameters based on the pre-scan size-specific dose estimate (SSDE). Eur Radiol. 2017;27:2267–74.
4. Kawashima H, Ichikawa K, Hanaoka S, et al. Relationship between size-specific dose estimates and image quality in computed tomography depending on patient size. J Appl Clin Med Phys. 2018;19(4):246–51.
5. Iriuchizima A, Fukushima Y, Nakajima T, et al. Simple method of size-specific dose estimates calculation from patient weight on computed tomography. Radiat Prot Dosim. 2018;178:208–12.
6. Karmazyn B, Ai H, Klahr P, Ouyang F, Jennings SG. How accurate is size-specific dose estimate in pediatric body CT examinations? Pediatr Radiol. 2016;46:1234–40.
7. Imai R, Miyazaki O, Horiuchi T, Kurosawa H, et al. Local diagnostic reference level based on size-specific dose estimates: assessment of pediatric abdominal/pelvic computed tomography at a Japanese national children's hospital. Pediatr Radiol. 2015;45:345–53.
8. Wang J, Duan X, Christner JA, Leng S, Yu L, et al. Attenuation based estimation of patient size for the purpose of size specific dose estimation in CT: Part I. development and validation of methods using the CT image. Med Phys. 2012;39:6764–71.
9. Wang J, Duan X, Christner JA, Leng S, Yu L, et al. Attenuation based estimation of patient size for the purpose of size specific dose estimation in CT: Part II. Implementation on abdomen and thorax phantoms using cross sectional CT images and scanned projection radiograph images. Med Phys. 2012;39:6772–8.
10. McCollough C, Bakalyar DM, Bostani M, Brady S, et al. Use of water equivalent diameter for calculating patient size and size-specific dose estimates (SSDE) in CT. Report of AAPM Task Group 220, 2014.
11. Li B, Behrman RH, Norbash AM. Comparison of topogram-based body size indices for CT dose consideration and scan protocol optimization. Med Phys. 2012;39:3456–65.
12. Anam C, Fujibuchi T, Toyoda T, Sato N, et al. A simple method for calibrating pixel values of the CT localizer radiograph for calculating water-equivalent diameter and size-specific dose estimate. Radiat Prot Dosim. 2018;179:158–68.
13. Zhang D, Mihai G, Barbaras LG, Brook OR, et al. A new method for CT dose estimation by determining patient water equivalent diameter from localizer radiographs geometric transformation and calibration. Med Phys. 2018;45:3371–8.
14. Koyanagi Y. The reduction of radiation exposure from ct examinations. Jpn J Occup Med Traumatol. 2015;63(4):219–24.